ELSEVIER

International Journal of Solids and Structures 41 (2004) 2331–2347

INTERNATIONAL JOURNAL OF SOLIDS and STRUCTURES

www.elsevier.com/locate/ijsolstr

Variational solutions to stresses in cracked cross-ply laminates under bending

Sunil Kuriakose [a], Ramesh Talreja [b,*]

[a] School of Aerospace Engineering, Georgia Institute of Technology, Atlanta, GA 30332, USA

[b] Department of Aerospace Engineering, Texas A&M University, HR Bright Building, College Station, TX 778433141, USA

Received 29 October 2003; received in revised form 29 October 2003

Abstract

Approximate analytical solutions based on a variational approach are presented for stresses in two cross-ply laminates, $[90_m/0_n]_s$ and $[0_m/90_n]_s$, with matrix cracks in the 90° layers, subjected to bending. The analysis assumes a plane stress state in longitudinal sections of the laminate and accounts for the lack of symmetry caused by partially closed crack planes or by cracks present on one side of the laminate mid-plane. Comparisons with finite element analysis for laminates of glass/epoxy and graphite/epoxy show that the stress components in the cracked layers in the regions of interest are in good agreement with analytical results. The model is therefore suitable for predicting matrix crack multiplication in addition to estimating the residual flexural stiffness. The results obtained show that the transverse normal stress at the 0/90 interface is compressive for $[0/90]_s$ laminate, while this stress is tensile in regions of the interface closer to the crack for the $[90/0]_s$ laminate. Thus the analysis suggests that delamination is possible under bending in the $[90/0]_s$ laminate.

1. Introduction

Composite laminates in structural applications are generally subjected to combinations of in-plane loads as well as bending and torsional moments. However, most studies in the past have focused on the laminate response under in-plane loads only, primarily under uniaxial loading parallel to a symmetry direction. Experimental observations of damage in symmetric laminates under tension parallel to a symmetry (axial) direction have shown that the damage occurs first in the form of transverse ply cracks, i.e. matrix cracks that run parallel to the fiber direction in off-axis plies. Subsequently, delamination occurs, more commonly under cyclic loading, in interfacial regions surrounding intersections of ply cracks in two neighboring plies. These damage modes and the associated laminate response have been studied extensively and reported widely in the literature (e.g., Reifsnider, 1977; Parvizi et al., 1978; Flaggs and Kural, 1982; Talreja, 1985a; Hashin, 1985; Wang et al., 1985; Laws and Dvorak, 1988; Whitcomb, 1992; Nairn and Hu, 1994). Among

* Corresponding author. Tel.: +1-979-458-3256; fax: +1-979-845-6051.
E-mail address: talreja@aero.tamu.edu (R. Talreja).

0020-7683/$ - see front matter © 2003 Published by Elsevier Ltd.
doi:10.1016/j.ijsolstr.2003.11.022

the approaches taken to analyze and model damage are the approximate one-dimensional shear-lag analysis (e.g., Highsmith and Reifsnider, 1982), variational and other solutions to local stresses (e.g., Hashin, 1985; Nairn, 1995; McCartney, 1996a,b) and continuum damage mechanics based approaches (e.g., Talreja, 1985b; Allen et al., 1987; Maire and Chaboche, 1997). The reader is referred to a recent publication for a detailed review of the developments in this area (Nairn, 2000).

The work to treat laminates undergoing damage in bending has begun only in recent years. Experimental investigations in this area have been reported by Echaabi et al. (1996) and Adolfsson and Gudmundson (1999). Smith and Ogin (1999) have obtained estimates of the reduced flexural modulus as a function of crack density based on the shear-lag approach. Li et al. (1994) have developed a semi-numerical approach to solve for the stresses in the cracked laminate under bending. Their approach is similar to the displacement based finite element method with discretization only in the thickness direction. The field variables are approximated by Fourier series expansions in the in-plane directions, thus allowing the stresses and effective properties for different crack spacings to be calculated by discretizing the domain only once.

Among more advanced analytical work on bending in laminates with transverse cracks is the method developed by McCartney and Pierse (1997) that provides approximate solutions to the stress state. In his approach the laminate is subdivided into several layers in the thickness direction and the 2-D elasticity equations for each layer with appropriate interface and boundary conditions are considered. Solution to the stress state is obtained by introducing approximating assumptions in the constitutive relations as well as in the boundary conditions. The accuracy of the results can be improved by increasing the number of layer subdivisions.

Another approach is that of Adolfsson and Gudmundson (1997) who developed a method to predict the reduced thermoelastic properties. This approach derives the work done by transverse cracking in a laminate by using the stress intensity factor for an array of parallel cracks in an infinite transversely isotropic medium. Although simple and generally applicable to symmetric laminates, as well as to cracking in multiple layers, there is uncertainty concerning the accuracy of this approach. The errors introduced by the assumption of a homogeneous infinite medium would presumably depend on how different the axial ply properties of the cracked ply are from those of the neighboring plies, as well as on the fact that the laminate thickness is finite and often only a few times as large as the crack length.

The objective of the work presented here is to analyze stresses in cross-ply laminates in which transverse ply cracks form under application of a bending moment. The cases considered are $[90_m/0_n]_s$ and $[0_m/90_n]_s$ laminates with cracks in the 90° layers. In both cases a variational approach used earlier for axial loading of cross-ply laminates (Hashin, 1985) is used. Kim and Nairn (2000) have used a similar approach to study the crack formation in the coating in coating/substrate systems under bending loads. The stresses determined by this approach are verified by a finite element analysis. Finally, based on these stresses an assessment is made of further transverse cracking under increasing bending moment as well as of formation of delamination.

2. Stress analysis

We assume that transverse cracks have been formed in a given cross-ply laminate under axial tension or under monotonic or reversed bending. Following this, we investigate the stress state generated within the laminate under application of a fixed bending moment. We assume that under this moment the cracks remain open only on the tension side of the laminate mid-plane. Thus any cracks lying on the compression side that were formed under axial tension or under reversed bending are assumed to close and transmit compressive stresses across their planes. We note that the laminate symmetry about the mid-plane in the undamaged state is lost in the damaged state under the applied bending moment. The following analysis will account for this loss of symmetry.

We assume that the stresses in the cracked laminate can be obtained by modifying the stress state of the undamaged laminate with unknown perturbation functions. Approximations are introduced in these functions to simplify the analysis. An admissible stress state for applying the principle of minimum complementary potential energy is obtained from the assumed stress state by satisfying the 2-D equilibrium equations and the boundary and interface conditions. Minimizing the complementary energy functional with respect to the unknown functions gives the Euler–Lagrange equations to be solved along with appropriate boundary conditions at the crack faces. Further analysis for the two cases of cross-ply laminates follows.

2.1. Case I: $[90_m/0_n]_s$

The laminate with matrix cracks for this case is shown in Fig. 1a. The cracks are considered to extend over the width of the laminate and the crack spacing is assumed to be uniform. We consider the region between two consecutive cracks with spacing equal to a, as shown in Fig. 1b. Plane stress condition in the X–Z plane is assumed and thereby stresses in the Y-direction due to Poisson's effect are ignored.

First we consider the undamaged laminate subjected to a constant bending moment M. Classical lamination theory is used to obtain the stress state in the laminate and the strain $\underline{\varepsilon}$ in the laminate is given by

$$\underline{\varepsilon} = \underline{D}^{-1}\underline{M}Z \tag{2.1}$$

where $\underline{D}$ is the flexural stiffness matrix of the laminate, $\underline{M}$ is the vector of moment resultants and Z is the distance of the considered point from mid-plane. Thus

$$\underline{M} = \begin{Bmatrix} M \\ 0 \\ 0 \end{Bmatrix} \tag{2.2}$$

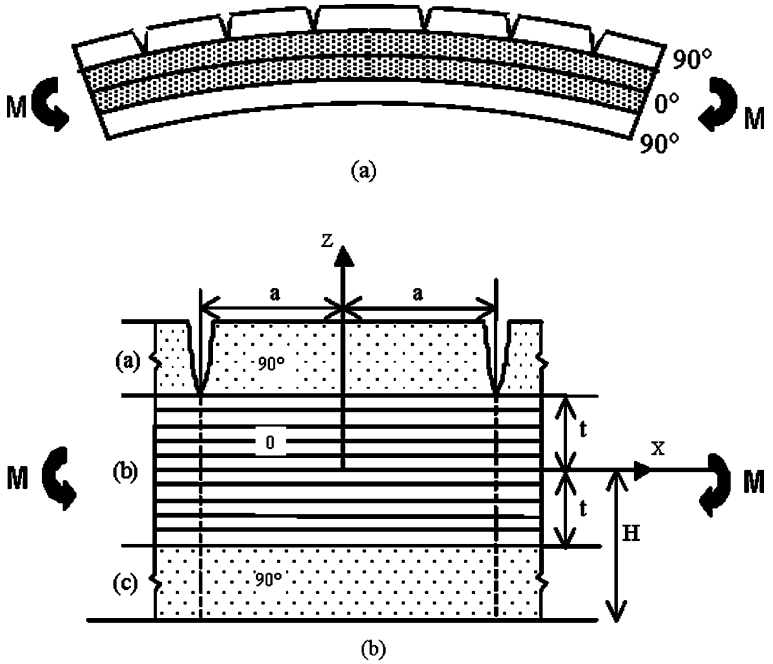

Fig. 1. (a) $[90_m/0_n]_s$ laminate with matrix cracks in 90° layer on the tension side and (b) Unit cell for stress analysis.

The stresses in the 90° and 0° layers are given by

$$\underline{\sigma}^{0(\alpha)} = \underline{Q}^{(\alpha)}\underline{\varepsilon} \tag{2.3}$$

where $\underline{Q}^{(\alpha)}$ is the reduced stiffness matrix for layer α which represents layer a, b, or c, as shown in Fig. 1b. The superscript 0 is used to indicate the stress for the undamaged laminate, which can be written as

$$\sigma_{xx}^{0(a)}(Z) = S_1 Z \tag{2.4a}$$

$$\sigma_{xx}^{0(b)}(Z) = S_2 Z \tag{2.4b}$$

$$\sigma_{xx}^{0(c)}(Z) = S_1 Z \tag{2.4c}$$

$$\sigma_{xz}^{0(a)}(Z) = \sigma_{xz}^{0(b)}(Z) = \sigma_{xz}^{0(c)}(Z) = 0 \tag{2.4d}$$

$$\sigma_{zz}^{0(a)}(Z) = \sigma_{zz}^{0(b)}(Z) = \sigma_{zz}^{0(c)}(Z) = 0 \tag{2.4e}$$

where

$$S_1 = \left[\sum_{j=1}^{3} Q_{1j}^{(90)} D_{j1}^{-1}\right] M \tag{2.5a}$$

and

$$S_2 = \left[\sum_{j=1}^{3} Q_{1j}^{(0)} D_{j1}^{-1}\right] M \tag{2.5b}$$

Here $\underline{Q}^{(0)}$ and $\underline{Q}^{(90)}$ are the reduced stiffness matrices of the 0° layer and the 90° layer, respectively. Integrating the moment due to the stresses given by (2.4) across the thickness the total bending moment M is obtained as

$$M = \tfrac{2}{3}(S_2 t^3 + S_1 H^3 - S_1 t^3) \tag{2.6}$$

where H and t are the thickness values as shown in Fig. 1b.

Now we consider the laminate with matrix cracks. The presence of cracks alters the stress field. Let $\sigma_{xx}^{C(\alpha)}(X,Z)$ be the total in-plane normal stress in layer α of the cracked laminate. Considering the new stress field as resulting from perturbations to the stresses of the undamaged laminate we can express the stresses in the cracked laminate as

$$\sigma_{xx}^{C(\alpha)}(X,Z) = \sigma_{xx}^{(\alpha)0}(Z) + \sigma_{xx}^{(\alpha)}(X,Z) \tag{2.7}$$

where $\sigma_{xx}^{(\alpha)}(X,Z)$ are the perturbation stress in the layer α.

The perturbation stresses are introduced in terms of unknown functions with the following simplifying assumptions

(i) The modified in-plane tensile stresses $\sigma_{xx}^{c(\alpha)}(X,Z)$ are linear in Z and depend on unknown functions of X.
(ii) Only the cracked layer (a) and the neighboring layer (b) are affected by the perturbation stresses.

With the above assumptions the perturbation to the in-plane normal stress in the cracked layer can be written as

$$\sigma_{xx}^{(a)}(X,Z) = -Z\widetilde{\phi}(X) + \widetilde{\psi}(X) \tag{2.8a}$$

and similarly for the layer (b)

$$\sigma_{xx}^{(b)}(X,Z) = -Z\tilde{\chi}(X) + \tilde{\eta}(X) \tag{2.8b}$$

where $\widetilde{\phi}(X)$, $\widetilde{\psi}(X)$, $\tilde{\chi}(X)$ and $\tilde{\eta}(X)$ are unknown functions to be determined. The functions $\widetilde{\psi}(X)$ and $\tilde{\eta}(X)$ that are constants in Z are introduced to take into account the effect of the loss of symmetry of the laminate geometry about the mid-plane. The stress in the layer (c) is taken as unaltered by the presence of the crack following the approximating assumption (ii) mentioned above. From (2.4), (2.7) and (2.8) the total in-plane normal stress in each layer is given by

$$\sigma_{xx}^{C(a)}(X,Z) = S_1 Z - Z\widetilde{\phi}(X) + \widetilde{\psi}(X) \quad t < Z < H \tag{2.9a}$$

$$\sigma_{xx}^{C(b)}(X,Z) = S_2 Z - Z\tilde{\chi}(X) + \tilde{\eta}(X) \quad -t < Z < t \tag{2.9b}$$

$$\sigma_{xx}^{C(c)}(X,Z) = S_1 Z \quad -H < Z < -t \tag{2.9c}$$

The following non-dimensional variables are introduced

$$\begin{aligned} &z = \frac{Z}{t} \quad x = \frac{X}{t} \quad h = \frac{H}{t} \\ &\phi(x) = \frac{t\widetilde{\phi}(X)}{\sigma_0} \quad \psi(x) = \frac{\widetilde{\psi}(X)}{\sigma_0} \\ &\chi(x) = \frac{t\tilde{\chi}(X)}{\sigma_0} \quad \eta(x) = \frac{\tilde{\eta}(X)}{\sigma_0} \end{aligned} \tag{2.10}$$

where $\sigma_0 = \sigma_{xx}^{0(a)}(t) = S_1 t$ is the stress in the 90° layer at the 0/90 interface in the undamaged laminate.

Using (2.10) we rewrite (2.8) with the non-dimensional variables as

$$\sigma_{xx}^{(a)}(x,z) = \sigma_0(-z\phi(x) + \psi(x)) \quad 1 < z < h \tag{2.11a}$$

$$\sigma_{xx}^{(b)}(x,z) = \sigma_0(-z\chi(x) + \eta(x)) \quad -1 < z < 1 \tag{2.11b}$$

The total laminate stresses are given as

$$\sigma_{xx}^{C(a)}(x,z) = \sigma_0 z + \sigma_0(-z\phi(x) + \psi(x)) \quad 1 < z < h \tag{2.12a}$$

$$\sigma_{xx}^{C(b)}(x,z) = \frac{S_2}{S_1}\sigma_0 z + \sigma_0(-z\chi(x) + \eta(x)) \quad -1 < z < 1 \tag{2.12b}$$

$$\sigma_{xx}^{C(c)}(x,z) = \sigma_0 z \quad -h < z < -1 \tag{2.12c}$$

Considering that the global load on the cracked laminate is the same as that before the cracks formed, the moment and force resultants computed with the new stress field should remain the same. Thus the following two conditions must be satisfied by the stresses. They are given as

$$\int_{-H}^{H} \sigma_{xx}^{C(\alpha)} Z \, \mathrm{d}Z = \int_{-H}^{H} \sigma_{xx}^{0(\alpha)} Z \, \mathrm{d}Z = M = \frac{2}{3}(S_2 t^3 + S_1 H^3 - S_1 t^3) \tag{2.13}$$

and

$$\int_{-H}^{H} \sigma_{xx}^{C(\alpha)} \, \mathrm{d}Z = \int_{-H}^{H} \sigma_{xx}^{0(\alpha)} \, \mathrm{d}Z = 0 \tag{2.14}$$

Two of the unknown perturbation functions can be eliminated by the application of the above conditions (2.13) and (2.14). Thus $\chi(x)$ and $\eta(x)$ can be expressed in terms of $\varphi(x)$ and $\psi(x)$ as follows:

$$\chi(x) = A_\phi \phi(x) + A_\psi \psi(x) \tag{2.15a}$$

$$\eta(x) = B_\phi \phi(x) + B_\psi \psi(x) \tag{2.15b}$$

where

$$A_\phi = -\tfrac{1}{2}(h^3 - 1) \tag{2.16a}$$

$$A_\psi = \tfrac{3}{4}(h^2 - 1) \tag{2.16b}$$

$$B_\phi = \tfrac{1}{4}(h^2 - 1) \tag{2.16c}$$

and

$$B_\psi = -\tfrac{1}{2}(h - 1) \tag{2.16d}$$

The stresses must satisfy the following equilibrium equations:

$$\frac{\partial \sigma_{xx}^{C(\alpha)}}{\partial X} + \frac{\partial \sigma_{xz}^{(\alpha)}}{\partial Z} = 0 \tag{2.17a}$$

$$\frac{\partial \sigma_{xz}^{C(\alpha)}}{\partial X} + \frac{\partial \sigma_{zz}^{(\alpha)}}{\partial Z} = 0 \tag{2.17b}$$

Introducing (2.12) into (2.17) and integrating gives the following expressions for the shear and normal stresses:

$$\sigma_{xz}^{(a)} = \sigma_0 \left[\frac{1}{2} z^2 \phi'(x) - z\psi'(x) \right] + f_a(x) \tag{2.18a}$$

$$\sigma_{xz}^{(b)} = \sigma_0 \left[\frac{1}{2} z^2 \chi'(x) - z\eta'(x) \right] + f_b(x) \tag{2.18b}$$

$$\sigma_{xz}^{(c)} = 0 \tag{2.18c}$$

$$\sigma_{zz}^{(a)} = \sigma_0 \left[-\frac{z^3}{6} \phi''(x) + \frac{z^2}{2} \psi''(x) \right] - z f_a'(x) + g_a(x) \tag{2.19a}$$

$$\sigma_{zz}^{(b)} = \sigma_0 \left[-\frac{z^3}{6} \chi''(x) + \frac{z^2}{2} \eta''(x) \right] - z f_b'(x) + g_b(x) \tag{2.19b}$$

and

$$\sigma_{zz}^{(c)} = 0 \tag{2.19c}$$

The functions $f_a(x)$, $f_b(x)$, $g_a(x)$ and $g_b(x)$ in (2.18) and (2.19) are to be determined using the following traction boundary and interface conditions:

$$\sigma_{xz}^{(a)}(x, h) = 0 \tag{2.20a}$$

$$\sigma_{xz}^{(b)}(x, 1) = \sigma_{xz}^{(a)}(x, 1) \tag{2.20b}$$

$$\sigma_{xz}^{(b)}(x,-1)=0 \tag{2.20c}$$

$$\sigma_{zz}^{(a)}(x,h)=0 \tag{2.20d}$$

$$\sigma_{zz}^{(b)}(x,1)=\sigma_{zz}^{(a)}(x,1) \tag{2.20e}$$

and

$$\sigma_{zz}^{(b)}(x,-1)=0 \tag{2.20f}$$

Eqs. (2.20) give six conditions to be satisfied but only four unknown functions are introduced by the integration. It can be shown that satisfying the equilibrium equations (2.17) along with the moment and force balance equations (2.13) and (2.14) ensures that imposing four of the above conditions identically satisfies the remaining two. Solving for the functions, the shear and normal stresses finally take the following form:

$$\sigma_{xz}^{(a)}=\sigma_0\left[-\frac{1}{2}(h^2-z^2)\phi'+(h-z)\psi'\right] \tag{2.21a}$$

$$\sigma_{xz}^{(b)}=\sigma_0\left[\frac{1}{2}(z^2-1)\chi'-(z-1)\eta'-\frac{1}{2}(h^2-1)\phi'+(h-1)\psi'\right] \tag{2.21b}$$

$$\sigma_{xz}^{(c)}=0 \tag{2.21c}$$

$$\sigma_{zz}^{(a)}=\sigma_0\left[\left(-\frac{z^3}{6}+\frac{h^2}{2}z-\frac{h^3}{3}\right)\phi''(x)+\frac{1}{2}(z-h)^2\psi''(x)\right] \tag{2.22a}$$

$$\sigma_{zz}^{(b)}=\sigma_0\left[\left(-\frac{z^3}{6}+\frac{1}{2}z-\frac{1}{3}\right)\chi''(x)+\frac{1}{2}(z-1)^2\eta''(x)+\left(-\frac{1}{3}(h^3-1)+\frac{1}{2}(h^2-1)\right)\phi''+\left(\frac{1}{2}(h^2-1)-(h-1)z\right)\psi''(x)\right] \tag{2.22b}$$

$$\sigma_{zz}^{(c)}=0 \tag{2.22c}$$

Note that $\phi(x)$ and $\psi(x)$ are the only unknowns in the stress state given by Eqs. (2.12), (2.21) and (2.22). This stress state satisfies the equilibrium equations and the traction boundary and interface conditions and therefore is an admissible stress state for applying the principle of minimum complementary energy. Hashin (1985) has shown that the complementary energy of the cracked laminate can be written in the form

$$\widetilde{U}_{\mathrm{c}}=U_{\mathrm{c}}^0+U_{\mathrm{c}}' \tag{2.23}$$

where U_{c}^0 is the complementary energy of the laminate without cracks and

$$U_{\mathrm{c}}'=\int_V S_{ijkl}\sigma_{ij}'\sigma_{kl}'\,\mathrm{d}V \tag{2.24}$$

Here σ_{ij}' are the perturbation stresses, S_{ijkl} is the compliance tensor and V is the laminate volume. Since U_{c}^0 is a known constant, minimizing U_{c}' with respect to $\phi(x)$ and $\psi(x)$ would give the required Euler–Lagrange equations to solve for the stress field.

The stress energy density for layer k of the laminate due to the perturbation stresses is given by

$$W^{(k)} = \frac{1}{2}\left(\frac{\sigma_{xx}^{(k)^2}}{E_{xx}} - \frac{2\nu_{xz}\sigma_{xx}^{(k)}\sigma_{zz}^{(k)}}{E_{xx}} + \frac{\sigma_{zz}^{(k)^2}}{E_{zz}} + \frac{\sigma_{xz}^{(k)^2}}{G_{xz}} \right) \tag{2.25}$$

Noting that the layers (a) and (b) have fibers running in y-direction and x-direction, respectively, the complementary energy densities of the layers are obtained as

$$W^{(a)} = \frac{1}{2}\left(\frac{\sigma_{xx}^{(a)^2}}{E_{\mathrm{T}}} - \frac{2\nu_{\mathrm{T}}\sigma_{xx}^{(a)}\sigma_{zz}^{(a)}}{E_{\mathrm{T}}} + \frac{\sigma_{zz}^{(a)^2}}{E_{\mathrm{T}}} + \frac{\sigma_{xz}^{(a)^2}}{G_{\mathrm{T}}} \right) \tag{2.26a}$$

$$W^{(b)} = \frac{1}{2}\left(\frac{\sigma_{xx}^{(b)^2}}{E_{\mathrm{A}}} - \frac{2\nu_{\mathrm{A}}\sigma_{xx}^{(b)}\sigma_{zz}^{(b)}}{E_{\mathrm{A}}} + \frac{\sigma_{zz}^{(b)^2}}{E_{\mathrm{T}}} + \frac{\sigma_{xz}^{(b)^2}}{G_{\mathrm{A}}} \right) \tag{2.26b}$$

The total complementary energy per unit width of the laminate is given by

$$U_{\mathrm{c}}' = t^2\left\{ \int_{-\rho}^{\rho}\int_{1}^{h} W^{(a)}\,\mathrm{d}x\,\mathrm{d}z + \int_{-\rho}^{\rho}\int_{-1}^{1} W^{(b)}\,\mathrm{d}x\,\mathrm{d}z \right\} \tag{2.27}$$

where $\rho = a/t$ is the non-dimensionalized crack spacing.

Substituting the expressions for the stresses from (2.12), (2.21) and (2.22) in (2.26) and performing the integration given by (2.27) over the thickness direction gives the complementary energy as a functional in $\phi(x)$ and $\psi(x)$. The expression for the complementary energy is thus obtained in the following form:

$$\begin{aligned} U_{\mathrm{c}}' = \int_{x=-\rho}^{x=\rho} t^2\Big[& P_{00}\phi(x)^2 + P_{02}\phi(x)\phi''(x) + P_{22}\phi''(x)^2 + P_{11}\phi'(x)^2 + R_{00}\psi(x)^2 + R_{02}\psi(x)\psi(x) + R_{22}\psi(x)^2 \\ & + R_{11}\psi(x)^2 + T_{00}\phi(x)\psi(x) + T_{02}\psi(x)\phi''(x) + T_{20}\phi(x)\psi''(x) + T_{22}\phi''(x)\psi''(x) + T_{11}\phi'(x)\psi'(x)\Big]\mathrm{d}x \end{aligned} \tag{2.28}$$

The coefficients P_{ij}, R_{ij} and T_{ij} in (2.28) are obtained by performing the z-direction integration in (2.27). They are functions of the elastic constants and the thickness ratio h. Performing the z-direction integration manually would be tedious but can be easily done using a symbolic computation software such as Maple and the coefficients P_{ij}, R_{ij} and T_{ij} can be obtained. Minimizing (2.28) with respect to $\phi(x)$ and $\psi(x)$ gives the following set of simultaneous ordinary differential equations

$$p_4\frac{\mathrm{d}^4\phi}{\mathrm{d}x^4} + s_4\frac{\mathrm{d}^4\psi}{\mathrm{d}x^4} + p_2\frac{\mathrm{d}^2\phi}{\mathrm{d}x^2} + s_2\frac{\mathrm{d}^2\psi}{\mathrm{d}x^2} + p_0\phi + s_0\psi = 0 \tag{2.29a}$$

$$q_4\frac{\mathrm{d}^4\psi}{\mathrm{d}x^4} + s_4\frac{\mathrm{d}^4\phi}{\mathrm{d}x^4} + q_2\frac{\mathrm{d}^2\psi}{\mathrm{d}x^2} + s_2\frac{\mathrm{d}^2\phi}{\mathrm{d}x^2} + q_0\psi + s_0\phi = 0 \tag{2.29b}$$

where

$$p_4 = P_{22} \quad p_2 = P_{02} - P_{11} \quad p_0 = P_{00}$$

$$q_4 = R_{22} \quad q_2 = R_{02} - R_{11} \quad q_0 = R_{00}$$

$$s_4 = \frac{T_{22}}{2} \quad s_2 = \frac{(T_{02} + T_{20} - T_{11})}{2} \quad s_0 = \frac{T_{00}}{2}$$

The above set of equations requires eight boundary conditions, four each on $\phi(x)$ and $\psi(x)$. The traction free condition on the crack plane gives the following conditions:

$$\sigma_{xx}^{(a)L}(\pm a, z) = 0 \tag{2.30a}$$

$$\sigma_{xz}^{(a)}(\pm a, z) = 0 \tag{2.30b}$$

In terms of $\phi(x)$ and $\psi(x)$ the conditions are

$$\phi(\pm a) = 1 \tag{2.31a}$$

$$\phi'(\pm a) = 0 \tag{2.31b}$$

$$\psi(\pm a) = 0 \tag{2.31c}$$

$$\psi'(\pm a) = 0 \tag{2.31d}$$

The solution to (2.29) is given by

$$\phi(x) = C_i e^{r_i x} \tag{2.32a}$$

$$\psi(x) = D_i e^{r_i x} \tag{2.32b}$$

where r_i are the eight solutions to the characteristic equation

$$(p_4q_4 - s_4^2)r^8 + (p_4q_2 + p_2q_4 - 2s_4s_2)r^6 + (p_4q_0 + p_0q_4 + p_2q_2 - 2s_4s_0 - s_2^2)r^4 + (p_2q_0 + p_0q_2 - 2s_2s_0)r^2 + (p_0q_0 - s_0^2) = 0 \tag{2.33}$$

C_i are the corresponding integration constants and D_i are given in terms of C_i as follows:

$$D_i = -\frac{s_4 r_i^4 + s_2 r_i^2 + s_0}{p_4 r_i^4 + p_2 r_i^2 + p_0} C_i$$

Eq. (2.33) gives solutions for r_i in the form $\pm(\alpha_i \pm \beta_i)$. The eight constants C_i are obtained by applying the boundary conditions (2.31).

2.2. Case II: $[0_m/90_n]_s$

Using the approach described above, an approximate solution to the stress state in the $[0_m/90_n]_s$ laminate with transverse cracks in the 90° layers on the tension side was also obtained. The following assumption regarding the width of the crack is made for this case. The crack is considered to extend in the range $0 < Z < t$ along the thickness of the laminate (Fig. 2). This may not be true in a real case. Under monotonic loading, the in-plane tensile stress being small near the neutral axis the crack may extend from the top 0/90 interface to some point above the neutral axis. Another case is that of the crack extending through the thickness of the 90° layer. This can occur under in-plane tensile loading or under cyclic bending. In this case, under a bending moment the crack will be open from the top 0/90 interface to a point below the neutral axis. However, the inaccuracy due to the above assumption is expected to be small, since the in-plane tensile stress is small near the neutral axis compared to locations away from the neutral axis. The perturbations to the in-plane tensile stresses are therefore taken as

$$\sigma_{xx}^{(a)}(X, Z) = -Z\tilde{\eta}(X) \quad t < Z < H \tag{2.34a}$$

$$\sigma_{xx}^{(b)}(X, Z) = -Z\widetilde{\phi}(X) \quad 0 < Z < t \tag{2.34b}$$

$$\sigma_{xx}^{(c)}(X, Z) = -Z\tilde{\chi}(X) \quad -t < Z < 0 \tag{2.34c}$$

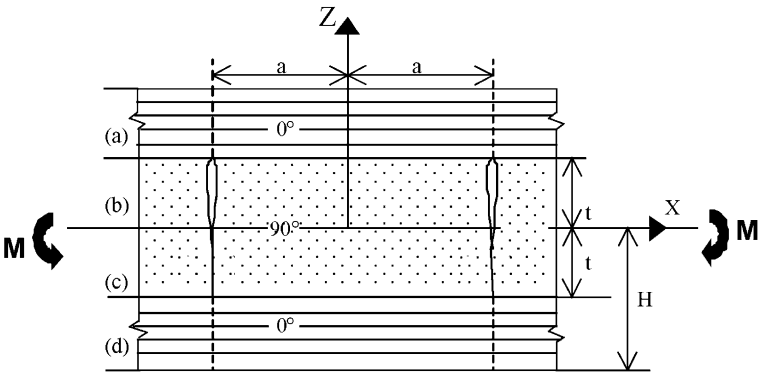

Fig. 2. Unit cell for a $[0_m/90_n]_s$ laminate with matrix cracks.

Superscripts (*a*), (*b*), (*c*) and (*d*) are used to indicate the stresses in the corresponding layer (see Fig. 2; layer (*b*) is the layer with cracks).

Following the procedure described for the case of $[90_m/0_n]_s$ laminates two of the unknown functions $\tilde{\eta}(X)$ and $\tilde{\chi}(x)$ can be eliminated and a closed form solution to $\tilde{\phi}(x)$ can be obtained.

Example cases for a $[90/0]_s$ and a $[0/90]_s$ glass/epoxy laminates are solved and comparisons with finite element computations are presented in Section 4.

3. Finite element modeling

The analytical models were validated by comparing with finite element computations on unit cells for a glass/epoxy and a graphite/epoxy laminate. The lamina properties used are given below.

Ply thickness, $t = 0.2$ mm.

Glass Epoxy : $E_A = 50.0$ GPa $E_T = 15.20$ GPa $\nu_A = 0.254$ $\nu_T = 0.428$ $G_A = 4.70$ GPa $G_T = 3.28$ GPa

Graphite Epoxy : $E_A = 130.0$ GPa $E_T = 9.70$ GPa $\nu_A = 0.300$ $\nu_T = 0.500$ $G_A = 5.00$ GPa $G_T = 3.60$ GPa

where subscripts 'A' and 'T' stand for axial and transverse directions, respectively.

The finite element computations were done using ABAQUS. A two-dimensional unit cell for a laminate with crack spacing equal to the thickness of the laminate ($4t$) was modeled using rectangular plane stress elements. The meshes used for $[90/0]_s$ and $[0/90]_s$ are shown in Figs. 3 and 4, respectively. The $[90/0]_s$ laminate mesh has 288 elements and 384 elements were used for $[0/90]_s$. In the case of $[0/90]_s$ laminate the crack was assumed to extend through the thickness of the 90° layer and contact elements were used at the crack face to simulate the closing of the crack on the compression side.

The traction distribution on the boundary of the unit cell corresponding to the applied bending moment is not known apriori. Therefore the analysis was done by an iterative approach to arrive at the correct boundary conditions along with the stress state. The iterative scheme used is described below.

The linear stress distribution in the cross-section of the undamaged laminate corresponding to a bending moment is known from classical laminate theory. This stress distribution is applied as the traction conditions on face B of the unit cell of the cracked laminate (Figs. 3 and 4). The unit cell being a repetitive

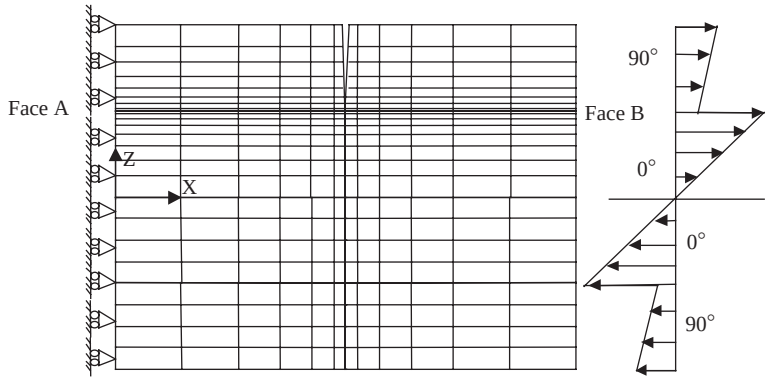

Fig. 3. Finite element model for $[90/0]_s$ unit cell.

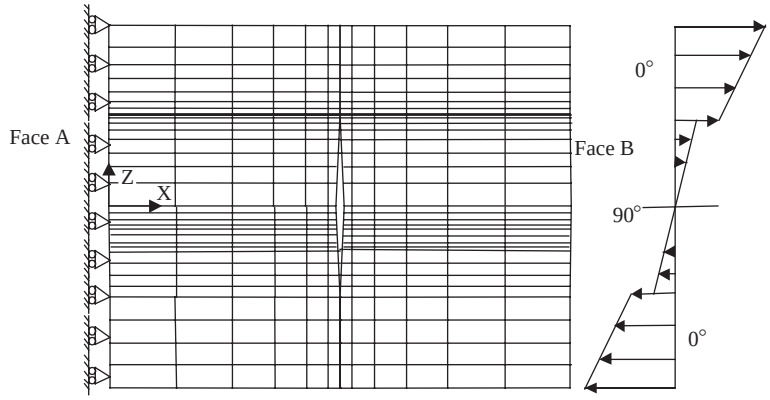

Fig. 4. Finite element model for $[0/90]_s$ unit cell.

element symmetry conditions are applied on face A. The finite element computation is performed and the traction distribution on the face A is obtained. This traction is applied on the face B and the finite element computation is repeated. The analysis is repeated this way until the difference between the tractions from two successive iterations becomes negligible. The stress field finally obtained is symmetrical and corresponds to the global moment applied on the laminate. In carrying out this procedure starting with the undamaged laminate stresses as the boundary condition the tractions at the symmetric face converged in three to four iterations.

4. Results and discussion

Comparisons of the stresses with the finite element (FE) results are shown in Figs. 5–12. The stress values are non-dimensionalized with respect to the axial stress in the 90° layer in the undamaged laminate at $Z = t$ (denoted by σ_0). Figs. 5 and 6 show the distribution of the inplane normal stress σ_{xx} across the thickness at $X = 0$, i.e., mid-way between two consecutive cracks, in glass/epoxy laminates of $[90/0]_s$ and $[0/90]_s$ layups, respectively. Stresses in this section are of interest because a new crack is likely to form along this section in

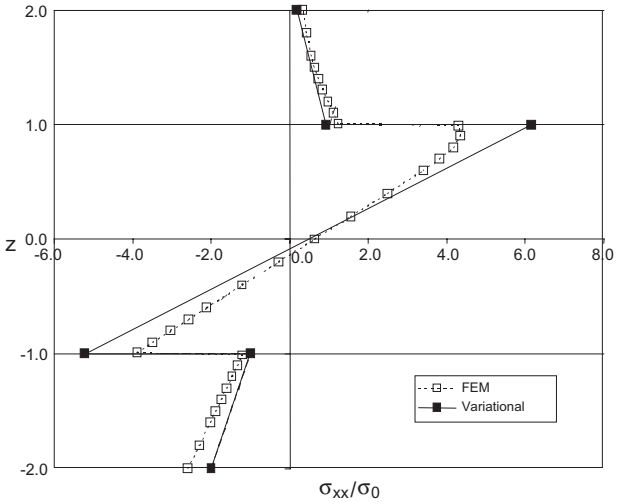

Fig. 5. $[90/0]_s$ glass/epoxy laminate: distribution of inplane normal stress across the thickness at $X = 0$ (mid-way between consecutive cracks).

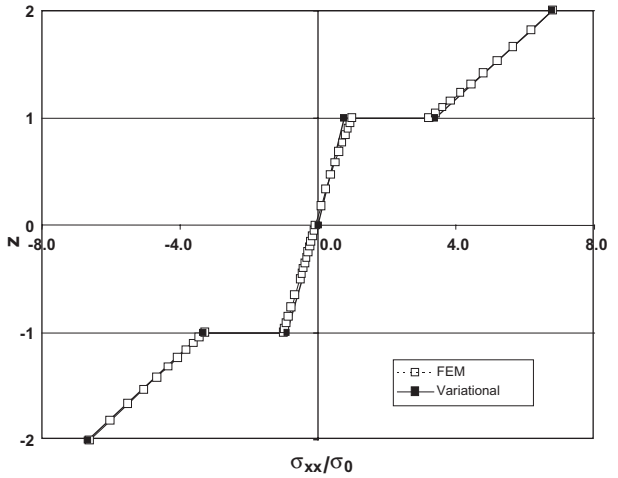

Fig. 6. $[0/90]_s$ glass/epoxy laminate: distribution of inplane normal stress across the thickness at $X = 0$ (mid-way between consecutive cracks).

the 90° layers (top layer in $[90/0]_s$ and the layer above the mid-plane in $[0/90]_s$). It can be seen that the predicted stresses and FE results match very well in these regions of the section. Fig. 7 shows the axial distribution of the three stress components in the cracked layer of $[90/0]_s$ glass/epoxy laminate at $Z = 1.5t$, i.e., mid-way through the thickness. Similar results for $[90/0]_s$ graphite/epoxy laminate are shown in Fig. 8. Figs. 9 and 10 show similar plots for the $[0/90]_s$ laminate at $Z = 0.5t$, i.e., mid-way through the thickness of the cracked 90° layer. Note that the stresses show good agreement for both laminates away from the crack planes.

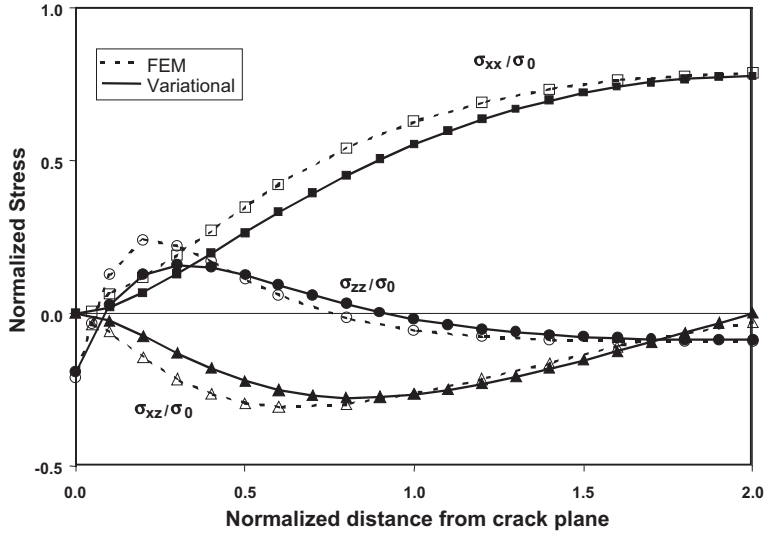

Fig. 7. $[90/0]_s$ laminate (glass/epoxy): axial distribution of stresses in the cracked layer at $Z = 1.5t$.

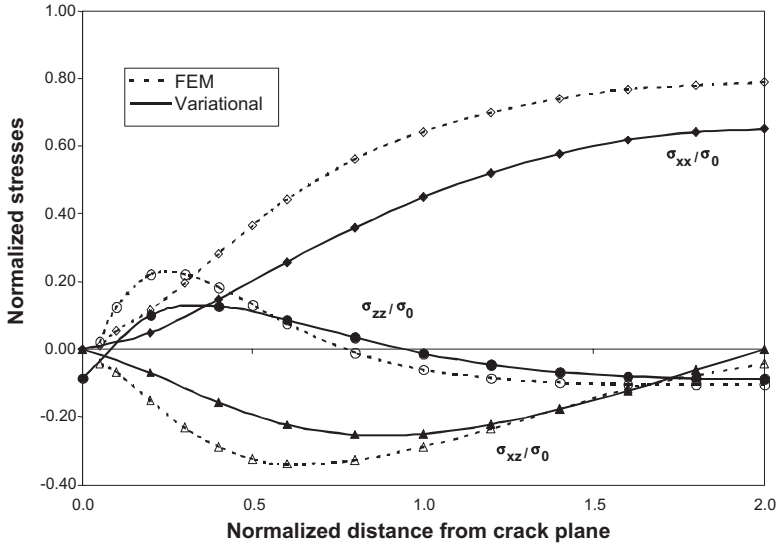

Fig. 8. $[90/0]_s$ laminate (graphite/epoxy): axial distribution of stresses in the cracked layer at $Z = 1.5$.

We shall now examine the stresses close to the 0/90 interface where interface cracks are likely to form. Figs. 11 and 12 show the axial distributions of stresses for graphite epoxy laminates at $Z = 1.1t$ for $[90/0]_s$ and at $Z = 0.9t$ for $[0/90]_s$. Similar results were obtained for glass/epoxy laminates. An interesting result is obtained. The transverse normal stress σ_{zz} is tensile close to the 0/90 interface in the vicinity of the crack tip for the $[90/0]_s$ laminate, while it is compressive for the $[0/90]_s$ laminate. Thus delamination is likely in the $[90/0]_s$ laminate.

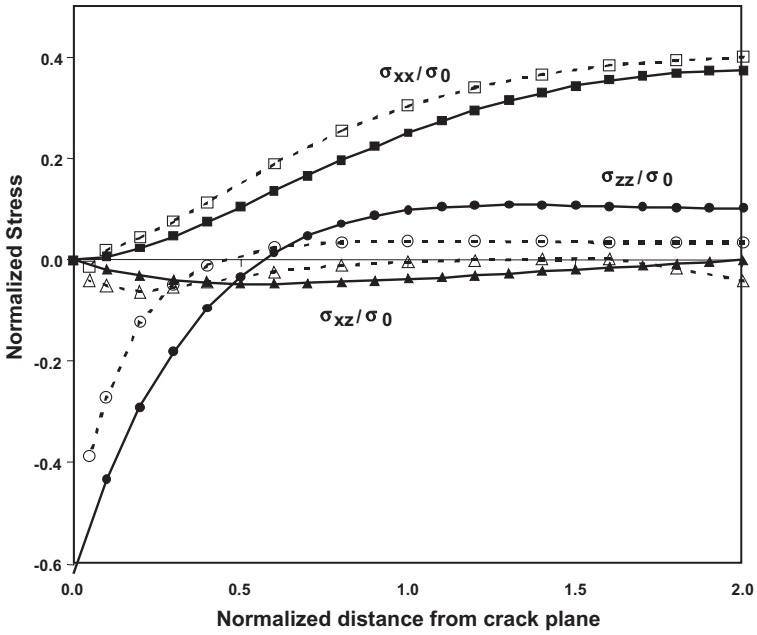

Fig. 9. $[0/90]_s$ laminate (glass/epoxy): axial distribution of stresses in the cracked layer at $Z = 0.5t$.

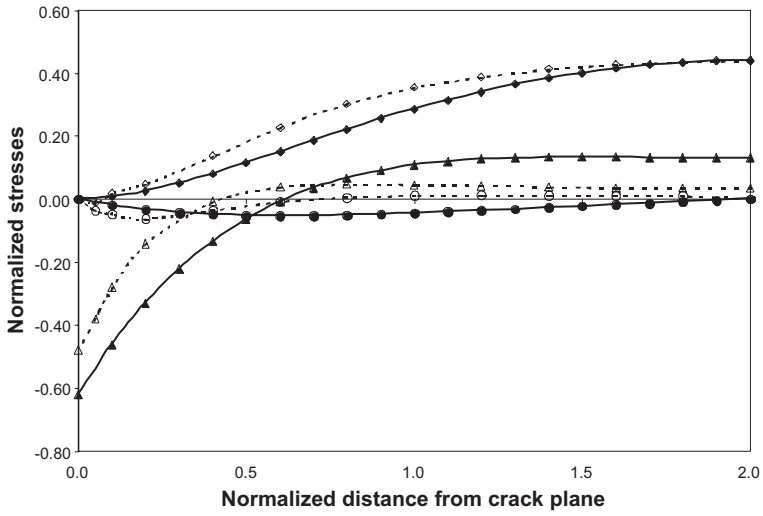

Fig. 10. $[0/90]_s$ laminate (graphite/epoxy): axial distribution of stresses in the cracked layer at $Z = 0.5t$.

The finite element results give high stress concentrations close to the crack tips, and these stresses would increase with mesh refinement as a consequence of the presence of stress singularity. The approximate stress field assumed in the variational approach does not take the crack tip stress singularity into account. However, the singularity is considered to be of no consequence for the evolution of transverse ply cracking,

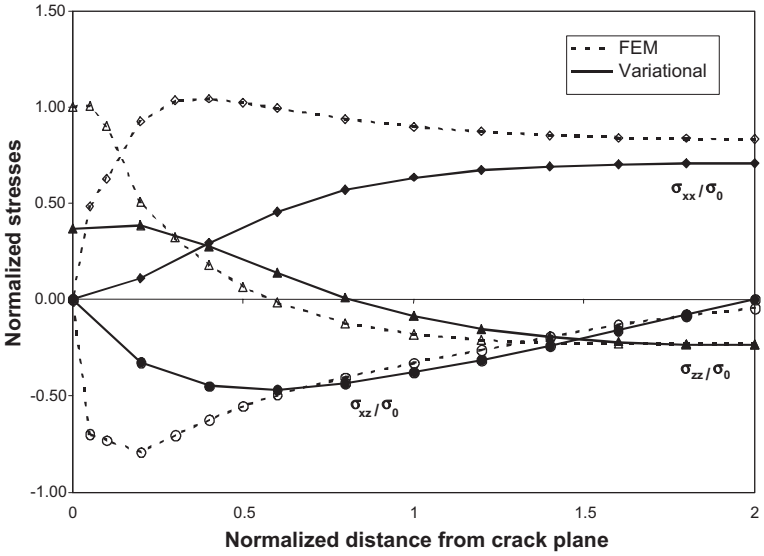

Fig. 11. $[90/0]_s$ laminate (graphite/epoxy): axial distribution of stresses in the cracked layer at $Z = 1.1t$.

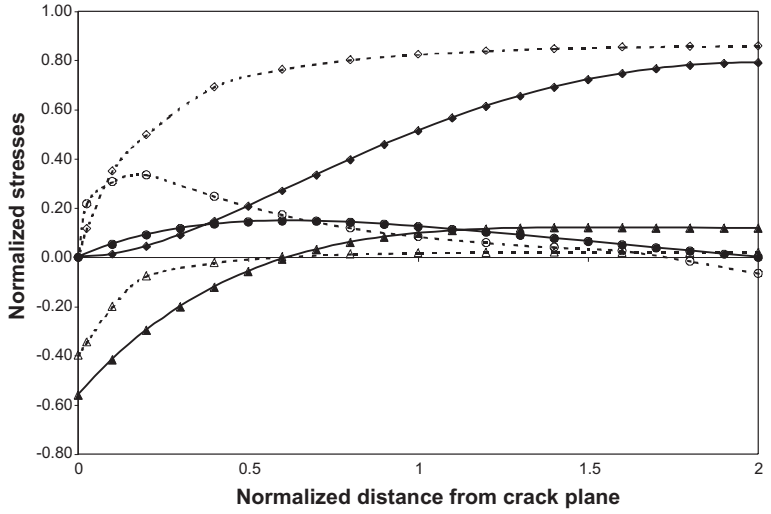

Fig. 12. $[0/90]_s$ laminate (graphite/epoxy): axial distribution of stresses in the cracked layer at $Z = 0.9t$.

which normally occurs by the formation of new cracks at locations away from already existing cracks. Furthermore, the material heterogeneity at the fiber scale would tend to lower the stress gradients, as argued by Hashin (1985) in assuming a constant through-thickness axial stress. Thus, for the purpose of predicting matrix crack multiplication the results from this analysis are expected to be of sufficient accuracy. The model results for the axial normal stress compare generally well with the FE results in the region of interest for glass–epoxy laminates and for graphite–epoxy laminates. However, in one case of graphite–epoxy $[90/0]_s$ laminate, at $Z = 1.5t$, a large discrepancy exists (Fig. 8). It is noted that crack formation is

expected at the interface, $Z = t$, close to which the agreement between the model and numerical results is acceptable (Fig. 11).

5. Conclusion

Approximate analytical solutions for stress states in $[90/0]_s$ and $[90/0]_s$ laminates under bending with transverse ply cracks in the 90° layers are obtained using the variational approach. Finite element simulations were done for the case of crack spacing equal to twice the thickness of the 90° layer, and these agreed well with the analytical predictions in the regions where the next set of cracks is likely to form. The model can be expected to give even better accuracy for larger crack spacing, but the accuracy for smaller crack spacing may need further study. For the case of uniform tension on cross-ply laminates, the saturation crack spacing has been found to be of the order of the thickness of the 90° layer (Garrett and Bailey, 1977). However, for bending, other modes of damage such as delamination near the transverse crack tips or fracture of 0° layer are likely before matrix crack saturation occurs. Thus very low crack spacing may not be reached in reality.

The stress results for the two cases show that the transverse normal stress can be tensile or compressive, depending on the laminate lay-up and location of the cracked layer. Thus a study of the evolution of cracking must also consider the possibility of internal delamination in assessing further matrix cracking.

The assumption that the stresses in the layers farther from the cracked layer are unaffected by the cracking introduces some error in the calculated stresses in those layers. On the other hand, the assumption simplifies the analysis and gives the possibility of extending the approach to more general ply lay-ups. Further work is underway in this direction and for studying the evolution of matrix cracking and delamination.

Acknowledgement

The support for this work by a grant from NASA Glenn research Center (Dr. Rod Ellis, Program Manager) is gratefully acknowledged.

References

Allen, D.H., Harris, C.E., Groves, S.E., 1987. A thermomechanical constitutive theory for elastic composites with distributed damage—theoretical development. Int. J. Solids Struct. 23 (9), 1301–1318.

Adolfsson, E., Gudmundson, P., 1997. Thermoelastic properties in combined bending and extension if thin composite laminates with transverse matrix cracks. Int. J. Solids Struct. 34 (16), 2035–2060.

Adolfsson, E., Gudmundson, P., 1999. Matrix crack initiation and progression in composite laminates subjected to bending and extension. Int. J. Solids Struct. 36, 3131–3169.

Echaabi, J., Trochu, F., Oham, X.T., Oullet, M., 1996. Theoretical and experimental investigation of failure and damage progression of graphite–epoxy composites in flexural bending test. J. Reinforced Plast. Compos. 15, 740–754.

Flaggs, D.L., Kural, M.H., 1982. Experimental determination of the in situ tansverse lamina strength in graphite/epoxy laminates. J. Compos. Mater. 16, 103–116.

Garrett, K.W., Bailey, J.E., 1977. Multiple transverse fracture in 90° cross-ply laminates if a glass fibre-reinforced polyester. J. Mater. Sci. 12, 157–168.

Hashin, Z., 1985. Analysis of cracked laminates: a variational approach. Mech. Mater. 4, 121–136.

Highsmith, A.L., Reifsnider, K.L., 1982. Stiffness-reduction mechanisms in composite laminates. In: Reifsnider, K.L. (Ed.) Damage in Composite Materials, ASTM STP 775, pp. 103–117.

Kim, S.-R., Nairn, J.A., 2000. Fracture mechanics analysis of coating/substrate systems. Parts I and II. Engng. Fract. Mech. 65, 573–607.

Laws, N., Dvorak, G.J., 1988. Progressive transverse cracking in composite laminates. J. Compos. Mater. 22, 900–916.

Li, S., Reid, S.R., Soden, P.D., 1994. A finite strip analysis of cracked laminates. Mech. Mater. 18, 289–311.

Maire, J.F., Chaboche, J.L., 1997. A new formulation of continuum damage mechanics (CDM) for composite materials. Aerospace Sci. Technol. 1997 (4), 247–257.

McCartney, L.N., 1996a. Stress transfer mechanics for ply cracking in general symmetric laminates. NPL Report CMMT(A)50.

McCartney, L.N., 1996b. Generalized framework for the prediction of ply cracking in any symmetric laminate subject to general inplane loading. NPL Report CMMT(A)51.

McCartney, L.N., Pierse, C., 1997. Stress transfer mechanics for multiple ply laminates subject to bending. NPL Report CMMT(A)51.

Nairn, J.A., 1995. Some new variational mechanics results on composite microcracking. In: Proceedings of the ICCM-10. Fatigue and Fracture, vol. I, pp. 423–438.

Nairn, J.A., 2000. In: Talreja, R., Manson, J.E. (Eds.), Comprehensive Composite Materials: Volume 2—Polymer Matrix Composites. Elsevier, Amsterdam, pp. 403–432.

Nairn, J.A., Hu, S., 1994. In: Talreja, R. (Ed.), Damage Mechanics of Composite Materials. Elsevier, Amsterdam, pp. 187–243.

Parvizi, A., Garrett, K.W., Bailey, J.E., 1978. Constrained cracking in glass fiber-reinforced epoxy cross-ply laminates. J. Mater. Sci. 13, 195–201.

Reifsnider, K.L., 1977. Some fundamental aspects of the fatigue and fracture response of composite materials. In: Proceedings of the 14th Annual Society of Engineering Science Meeting, Lehigh University, Bethlehem, PA, November 14–16.

Smith, P.A., Ogin, S.L., 1999. On transverse matrix cracking in cross-ply laminates loaded in simple bending. Compos.: Pt. A 30, 1003–1008.

Talreja, R., 1985a. Transverse cracking and stiffness reduction in composite laminates. J. Compos. Mater. 19, 355–375.

Talreja, R., 1985b. A continuum mechanics characterization of damage in composite materials. Proc. R. Soc. London A 399, 195–216.

Wang, A.S.D., Kishore, N.N., Li, C.A., 1985. On crack development in graphite–epoxy $(0_2, 90_n)_s$ laminates under uniaxial tension. Compos. Sci. Technol. 24, 1–31.

Whitcomb, J.D., 1992. Analysis of delamination growth near intersecting ply cracks. J. Compos. Mater. 26, 1844–1858.